Influence of uterine cervix shape on photodynamic therapy efficiency

Artur Bednarkiewicz
Wieslaw Strek
Institute of Low Temperature and Structure Research
Polish Academy of Science
Ul. Okolna 2
50-422 Wroclaw, Poland
E-mail: abednar@int.pan.wroc.pl

Abstract. The goal of practical photodynamic therapy (PDT) dosimetry is to optimize the distribution of a light dose delivered to tissue by selecting the irradiation time and geometry to match the geometry and optical properties of the tumor and surrounding tissue. Homogeneous irradiation is among one of the sources of correct PDT dosimetry. The goal of this study is to model and predict the influence of the shape of a treated organ in need of light dose correction. Thus efficiency of light delivery to the tissue volume is defined and calculated with shape factors of the uterine cervix as parameters. Two cases (parallel and divergent beam) of enlightening configuration are investigated. The calculations presented extend PDT dosimetry with the influence of the shape of the uterine cervix on PDT necrosis depth. This allows for photodynamic excitation light dose correction for more reliable treatments. © *2004 Society of Photo-Optical Instrumentation Engineers.*
[DOI: 10.1117/1.1779626]

Keywords: dosimetry; photodynamic therapy; uterine cervix; biomedical optics.

Paper 03043 received Apr. 11, 2003; revised manuscript received Jul. 14, 2003, and Oct. 7, 2003; accepted for publication Jan. 16, 2004.

1 Introduction

Photodynamic therapy (PDT) and diagnosis (PDD) has become a recognized therapy and diagnostics tool for cancer treatment. This technique requires coexistence of at least three agents. A photosensitizer (PS), under light of proper fluence and wavelength, transforms chemical compounds (e.g., molecular oxygen O_2) to free radicals, which are directly responsible for local toxicity. Nevertheless, the efficiency of the treatment procedure is a complicated relation of the fluence of activating light, the initial concentration of the photosensitizer, and the fill-in coefficient of PS. For porphyrin derivatives and some other sensitizers, proper concentration of oxygen is required. In addition, these quantities and conditions may change during the treatment, due to photobleaching of the sensitizer, consumption of oxygen, variation of PS concentration, and others. The efficiency may also be patient and drug specific. In gynecological PDT, the menstrual cycle affects the fluorescence spectroscopy as a monitoring tool for dosimetry and diagnosis.[1]

Calculating the excitation light dosage, one should then consider several aspects. Higher irradiance may cause thermal effects in the tissue, as well as rapid consumption of oxygen leading to photobleaching and phototransformation of the photosensitizer.[2,3] These may decrease the effective concentration of the sensitizer, thus higher efficiency of the treatment must be obtained either by extending the time of treatment (lowering irradiance) or exciting by a fractionated light source.[4,5] The photochemical modification of PS and oxygen consumption should also be considered during prolonged light exposure.

There is also a need to develop sensitizers absorbing longer wavelengths because of the deeper penetration of light into tissue not affected by hemoglobin absorption.

Moreover, radiation dosage absorbed by photosensitisers strongly depends on the enlightening configuration and uniformity of light coming directly from a source[6] or from a light applicator,[7,8] as well as on the structure and morphology of the surface.

As we show, the complicated shape of the organ may also impact severely the efficiency of light penetration into the tissue, affecting all successive steps of the treatment procedure due to the nonhomogenous light dose delivery. There are not many attempts that consider the impact of the shape of the organ on the performance of PDT.[9,10]

There are two stages in the approach to PDT dosimetry. The first one is an attempt of direct measurement of drug concentration, light fluence, and oxygen concentration *in vivo* for individual patients. The measurement of these values is presently a challenge in ambulatory conditions. However, developing theoretical or phenomenological models or using neural networks may allow for prediction of the progress and monitoring of the treatment. There were also some approaches to build dosimetry theoretical models.[11–15] Starting from the theory of diffusion of light in tissue, Grossweiner developed a theory allowing the calculation of necrosis depth (z_n) for different geometries of excitation.[12]

The aim of the study was to estimate the light dose efficiency and necrosis depth reduction with the physiological shape of the uterine cervix as an input parameter. The more real configuration of enlightening the uterine cervix with a microlens fiber (divergent light) was also examined qualitatively and compared with a parallel light configuration. The potential clinical application of the model will allow us to

Address all correspondence to Artur Bednarkiewicz, Polish Academy of Sciences, Institute of Low Temperature and Structure Research, Polish Academy of Science, ul.Okolna 2, PL-50-950 Wroclaw, Poland. Tel: (48-071)-34-35-021-029 int. 188; FAX: (48-071)-34-41-029; E-mail Abednar@int.pan.wroc.pl
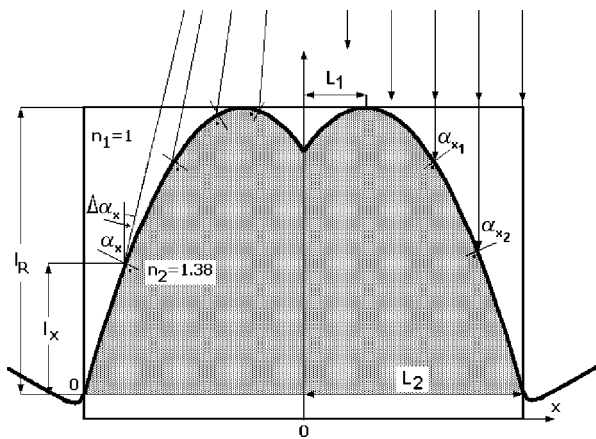
Fig. 1 The model profile of the uterine cervix. L_2 [mm] is a radius of the uterine cervix used as a base for relative height measurement I_R [mm], and L_1 [mm] is a radius at the top of the uterus. The left side of the figure presents rays from a divergent light source at distance L_3 [mm] from the top of the uterine cervix. In spite of incidence angle α_x to the normal of the surface at the x position, the $\Delta \alpha_x$ deflection angle is also observed in this case. The right side of the figure presents the case with parallel rays $(L_3 = \infty)$.

predict the additional time of light therapy or to improve light delivery for better effectiveness of PDT.

2 Methods

Let us assume in the first approximation that the uterine cervix is symmetrical in the shape. Let the I_R, L_1, and L_2 parameters describe the shape and the convexity of the organ. The meaning of these parameters is described in Fig. 1. Note that they can be estimated or measured before treatment procedure to correct light dose.

There are several factors to include for calculating the effectiveness η of therapeutical light delivery to the nonflat surface tissue volume. The first one is *Fresnel losses* due to the difference in the index of refraction on the air-tissue border. This factor is sensitive to the angle of incidence α_x of radiation versus normal to the tissue surface (see Fig. 1). The second factor—deflection angle $\Delta \alpha_x$—arises from divergency of the light source and impacts Fresnel losses as well. For the third factor, one should also consider the impact of the angle of incidence of the radiation versus normal to the surface ($\alpha_x + \Delta \alpha_x$ angle, see Fig. 1) on the *effective irradiance*. This will further reduce the incident irradiance by the $\cos(\alpha_x + \Delta \alpha_x)$ factor, especially for x close to L_2. For a point light source, the distance between the light source and the tissue surface also affects the effective irradiance. This results from lowering the optical power per area, while increasing the distance between the light source and the enlightened surface.

There is another factor influencing the effective incident irradiance, which in some cases cannot be neglected, but is difficult to consider quantitatively. The light, which is reflected and backscattered from the uterine cervix surface due to the Fresnel law, may undergo scattering or reflection from the surrounding vaginal tissue. The distance between the tissues during treatment is not close enough to play a major role in the irradiation (for the x close to L_2 case), however, one should be conscious about that process. The region (x close to

L_2) suffers most from the decrease of irradiance. This is the hint for improving uniformity of light distribution for uterine cervix photodynamic cancer treatments.

One should also be conscious about nonideal roughness of the surface of the uterine cervix. This factor is very difficult to consider quantitatively due to patient-to-patient changes. Another factor not considered within the presented model is the intensity profile of the light source. We use an approximation of the top-hat intensity profile, which in some cases is not a real one.

Let us now quantitatively consider the Fresnel losses and the effective irradiance factors by introducing the effectiveness of light delivery to the tissue volume η into the Grossweiner's model, where relation for necrosis depth is expressed as

$$z_n = \delta \cdot \ln \left[\eta \frac{E_0 t}{q^*} (3 + 2bR_d) \right]. \quad (1)$$

The δ is the penetration depth, where energy density decreases down to $1/e$ of the initial value on the surface ($E_o t$). The δ parameter depends on the wavelength of excitation and kind of tissue, but does not include absorption by blood. The knowledge of its value is critical for proper necrosis depth assessment, which has typical values of 1 to 3 mm for nonpigmented tissues in the red and near-IR spectral regions. The spectroscopic and optical properties of uterine cervix found in the literature[16] enabled us to calculate $R_d = 0.361$ and the penetration depth $\delta = 10.8$ mm, which seems quite high. The $3 + 2bR_d$ depends on the tissue optical constants and the mismatch between the refractive index of the tissue and the air. The $b = 3.115$ parameter was obtained for a typical value of index of refraction ($n = 1.38$) of tissue and internal reflectance coefficient ($r_i = 0.514$). The threshold energy fluence parameter q^* [Jm^{-2}] strongly depends on the type and concentration of PDT drug and wavelength used. Unfortunately, photobleaching or pharmacokinetics also has a negative impact on its value.

The local enhancement of irradiance under the uterine cervix epidermis surface coming from scattering is considered by the application of diffuse reflection coefficient (R_d) in the dosimetry model described by Eq. (1).

However, to make the calculation of scaled necrosis depth (z_n / δ) independent of the spectroscopic and optical properties of tissue, after applying simple relation $\ln(ab) = \ln(a) + \ln(b)$ to Eq. (1) and calculating the difference between flat (no Fresnel loss) and convex surface cases, one obtains

$$\Delta \frac{z_n}{\delta} = \left[\frac{z_n}{\delta} \right]_{convex} - \left[\frac{z_n}{\delta} \right]_{flat} = \ln \eta = \ln(\eta_F \cdot \eta_C \cdot \eta_L), \quad (2)$$

which is the scaled necrosis depth difference between convex and flat, no-loss enlightening configurations. This value informs us about the relative reduction of scaled necrosis depth ($\ln \eta$) or light dose loss ($1 - \eta$), as the uterine cervix becomes convex more and more. The η value is a product of Fresnel efficiency η_F and effective irradiance correction factors η_C and η_L. The η_C is the effective irradiance correction factor resulting from cosinus of the angle between the light

ray and the tissue surface. The η_L corrects the effective irradiance due to change of distance between the point light source and the tissue surface.

2.1 Fresnel Losses

The *Fresnel losses* are due to the difference in the index of refraction on the air-tissue border. The losses change with the angle of light incidence α_x on the tissue surface. To calculate this angle, starting from boundary conditions, one can write an equation of a parabola in the $x = 0 ... L_2$ range (see Fig. 1). Assuming the symmetry of uterine cervix, the Eq. (3). describes its shape:

$$I(x,I_R,L_1,L_2) = -\frac{I_R}{(L_1-L_2)^2}$$
$$\cdot [x^2 - 2L_1 x + L_2(2L_1 - L_2)]. \quad (3)$$

Calculating the first derivative of Eq. (3), one can easily obtain an angle of incidence of radiation versus normal to the surface α_x.

$$\alpha_x = \arctan[I'(x,I_R,L_1,L_2)]$$
$$= \arctan\left[-\frac{2 \cdot I_R}{(L_1-L_2)^2} \cdot (x-L_1) \right]. \quad (4)$$

This is true for a parallel light beam. Using a microlens fiber, one changes the angle of incidence (see Fig. 1). The calculation of deflection requires knowing the numerical aperture (NA) of the microlens and distance L_3 from fiber tip to the top of the uterine cervix. It was assumed that NA allows covering the circular area with the radius $L_2 = 25$ mm for arbitrary distance $L_3 + I_R$. The deflection angle (see Fig. 1) can be then written as

$$\Delta \alpha_x = \arctan\left[\frac{x}{L_3 + I_R - I_x} \right]. \quad (5)$$

For small x, one obtains

$$\lim_{L_3 = \infty} \Delta \alpha_x = 0,$$

which is the parallel case. The calculations presented in the work for the divergent case are in fact the application of a point light source located at $x = 0$ and at distance L_3 from the top of the uterine cervix.

Using the Fresnel equation (see the Appendix in Sec. 5), which describes the amplitude relations of reflected to deflected beams depending on the angle of incidence, one can calculate the absolute transmission coefficient η_F (Fresnel efficiency) through the border between air and tissue.

$$\eta_F(x,I_R,L_1,L_2) = n\left(\frac{A_D}{A_I} \right)^2, \quad (6)$$

where A_D and A_I are amplitudes of deflected and incident rays, respectively, which are obtained from Fresnel equations for nonpolarized light. The n factor is a relative index of refraction. Because the beam goes through the border between air ($n \sim 1$) and tissue ($n = 1.38$ mean value for tissues), there is no danger for total internal reflection. The η_F versus dis-

tance x, with convexity (I_R) and divergence (L_3) of a light source as parameters, is presented in Fig. 2(a). The Fresnel efficiency $\eta_F(x)$ includes both incidence (α_x) and deflection angles ($\Delta \alpha_x$).

2.2 Effective Irradiance

The effective irradiance efficiency η_I depends on two factors. The first one is the *cosinus factor* η_C, describing the dependence of the irradiance on the angle between the incident ray and the normal to the surface:

$$\eta_C = \cos(\alpha_x + \Delta \alpha_x), \quad (7)$$

for parallel beam source $\Delta \alpha_x = 0$. The dependence of the η_C versus distance x, with convexity (I_R) and divergence (L_3) of light source as parameters, is presented in Fig. 2(b).

The second factor, *power density* factor η_L, involves the distance between the light source and the tissue surface. It was assumed that at a distance $L_3 + I_R$ (the bottom of the uterine cervix), a point light source produces a cone with a radius of $L_2 = 25$ mm. The radius of a circular base of the cone for an arbitrary x position (see Fig. 1) is $R_{Ix} = L_2(L_3 + I_R - I_x)/(L_3 + I_R)$, where $I_x = I(x,I_R,L_1,L_2)$. The area calculated at the top ($I_x = I_R$) versus the area at I_x height from the bottom of the uterine cervix was used for the power density correction factor η_L construction:

$$\eta_L = \left(\frac{R_{I_R}}{R_{I_X}} \right)^2 = \frac{L_3^2}{(L_3 + I_R - I_x)^2}. \quad (8)$$

The dependence of the η_L versus distance x, with convexity (I_R) and divergence (L_3) of light source as parameters, is presented in Fig. 2(c). At the top of the uterine cervix ($I_x = I_R$) $\eta_L = 1$.

3 Results

Combining Eqs. (6), (7), and (8) into Eq. (2), one can present dose efficiency η [Figs. 3(a) and 3(b)] or scaled necrosis depth reduction $\Delta(z_n/\delta) = \ln \eta$ [Figs. 3(c) and 3(d)] versus the distance from the axis of symmetry.

Assuming that acceptable dose losses are 20% ($\eta = 0.8$), one obtains from Figs. 3(a) and 3(b) that only the top of the uterine cervix is efficiently enlightened. The 20% dose loss gives about 22% of scaled necrosis depth reduction. A radius of acceptance is equal to 7.7, 8.8, and 9.4 mm for $I_R = 25$ mm and a little larger, e.g., 10.5, 13.7, and 15.9 mm for $I_R = 10$ mm. This points out the urgent need for a reliable uterine cervix PDT light dose delivery illuminator.

The considerations are general, but it is easy to apply them to clinical cases, when exact values of spectroscopic and optical properties of treated tissue are known. One should add the $\Delta z_n/\delta$ value to the scaled necrosis depth calculated for a specific case. This will allow for correction of the exposure time for proper photodynamic treatment.

To make the obtained result even more general, dose efficiency $\eta' = \eta_F \eta_C$ [Fig. 4(a)] and scaled necrosis depth reduction $\Delta(z_n/\delta) = \ln \eta' = \ln \eta_F \eta_C$ [Fig. 4(b)] were presented versus the angle of incidence. The η_L was excluded from calculations due to an organ shape-specific dependence. The
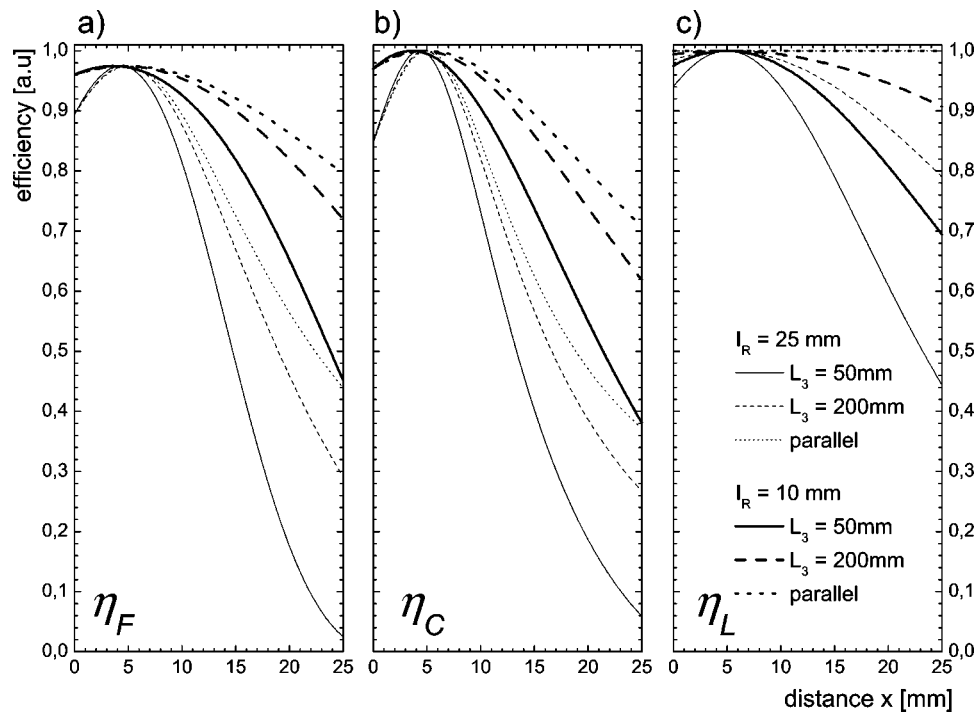
Fig. 2 (a) The profile of the Fresnel efficiency η_F, (b) cosinus factor η_C, and (c) power density factor η_L versus distance x from the axis of symmetry with the light beam of L_3 divergence and convexity of the uterine cervix (I_R) as parameters. $L_1 = 5$ mm and $L_2 = 25$ mm remain constant. Indexes of refraction $n_1 = 1$ and $n_2 = 1.38$ were used for calculations. Thin and thick lines represent convexity $I_R = 25$ and $I_R = 10$ mm, respectively. The solid, dashed, and dotted lines represent divergence $L_3 = 50$ mm, $L_3 = 200$ mm, and $L_3 = \infty$ (parallel case), respectively.
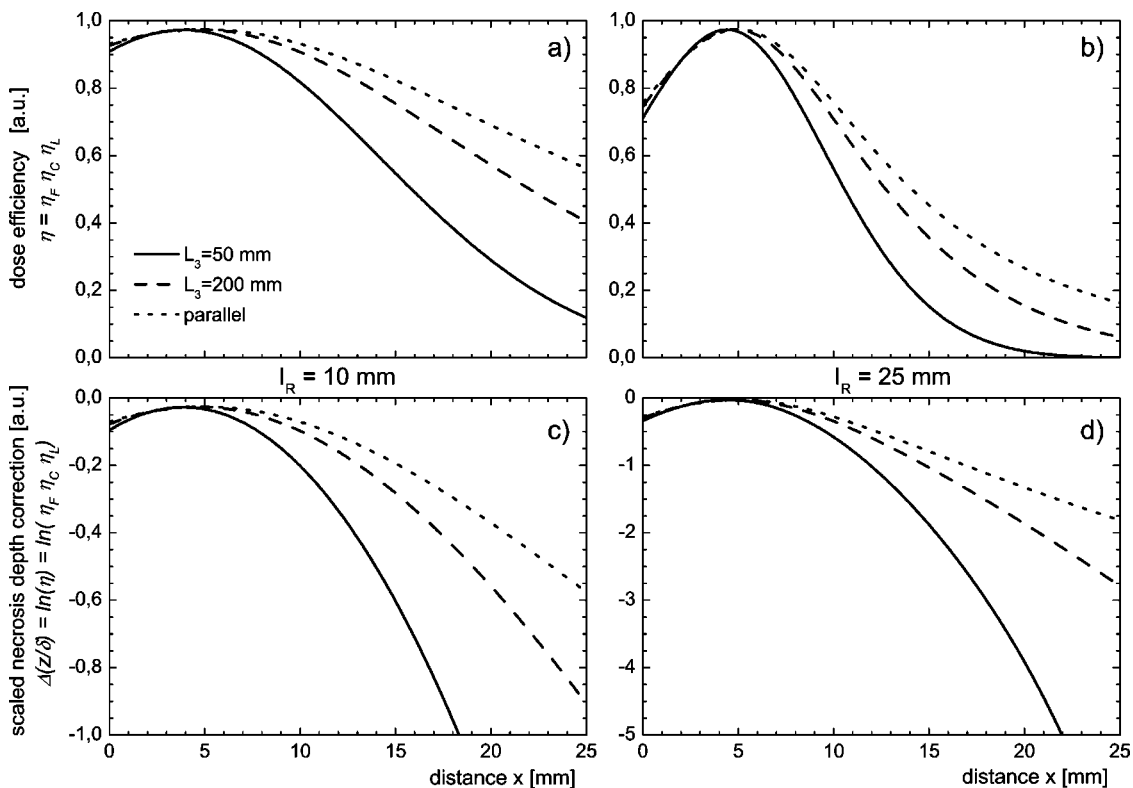
Fig. 3 The profiles of the dose efficiency η [(a) $I_R = 10$ mm, and (b) $I_R = 25$ mm] and the scaled necrosis depth reduction $\Delta(z_n/\delta) = \ln \eta$ [(c) $I_R = 10$ mm, and (d) $I_R = 25$ mm] versus the distance from the axis of the symmetry for different divergence of the light beam. The solid, dashed, and dotted lines represent divergence $L_3 = 50$ mm, $L_3 = 200$ mm, and $L_3 = \infty$ (parallel case), respectively. $L_1 = 5$ mm, $L_2 = 25$ mm, and $I_R = 25$ mm remain constant.
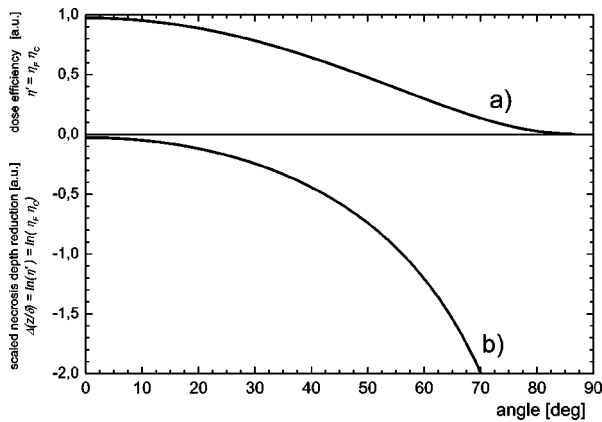
Fig. 4 (a) The profiles of the dose efficiency $\eta' = \eta_F \, \eta_C$ and (b) the scaled necrosis depth reduction $\Delta(z_n/\delta) = \ln \eta' = \ln(\eta_F \, \eta_C)$ versus an angle of incidence between a light ray and normal to the tissue surface.

obtained relations are independent from I_R, L_1, L_2, and L_3 parameters, which in fact narrow down the angle range for a specific tissue shape.

The 20% dose loss ($\eta' = 0.8$) gives around 22% of scaled necrosis depth reduction, which occurs for around a 30-deg angle between the incident ray and tissue surface.

4 Conclusions

We demonstrate the influence of the shape of an enlightened organ on the efficiency of PDT treatment defined as a necrosis depth reduction and dose efficiency. Using the curvature of the uterine cervix, we model the light dose delivery efficiency η on the border between air and tissue in the two enlightening configurations. The relative simplicity of the uterine cervix shape assessment (L_1, L_2, and I_R in Fig. 1) and relative simplicity of the mathematical procedure of the correction coefficient calculation allows for direct considerations in patient-specific effectiveness of light therapy. The results are general, because the real degree of correction is organ- and enlightening-configuration specific. The relations developed in the work allow us to assess the increase of treatment time needed for successive treatment due to the shape of the cervix. The considerations can be used for light applicator modeling and construction, and for enhancement of therapeutical procedures.

5 Appendix A

The Fresnel relation for deflected rays is expressed as

$$\left(\frac{A_D}{A_I}\right)^2 = \left[\frac{2\cos\alpha \cdot \sin\beta}{\sin(\alpha+\beta)\cos(\alpha-\beta)}\right]^2$$
$$\cdot\left[\cos^2\varphi + \sin^2\varphi\,\cos^2(\alpha-\beta)\right], \qquad (9)$$

where A_D and A_I are amplitudes of deflected and incident

rays, respectively, and the α and β variables are angles of incidence and deflection, respectively. For nonpolarized light, $\cos^2\varphi = \sin^2\varphi = 0.5$. The β angle was calculated (as a function of angle of incidence α) from the known relation

$$\frac{\sin\beta}{\sin\alpha} = \frac{n_1}{n_2}. \qquad (10)$$

The angle of incidence α depends on the curvature of the cervix (I_R), current position x from the axis, and the enlightening configuration (see Fig. 1).

References

1. S. K. Chang, M. Y. Dawood, G. Staerkel, U. Utzinger, E. N. Atkinson, R. R. Richards-Kortum, and M. Follen, "Fluorescence spectroscopy for cervical precancer detection: Is there variance across the menstrual cycle?," *J. Biomed. Opt.* **7**(4), 595–602 (2002).
2. R. Rotomskis, G. Streckyte, and S. Bagdonas, "Phototransformation of sensitisers 1. Significance of the nature of the sensitiser in the photobleaching process and photoproduct formation in aqueous solution," *Photochem. Photobiol.* **39**, 167–171 (1997).
3. R. Rotomskis, S. Bagdonas, G. Streckyte, R. Wenderburg, W. Dietel, J. Dzidziapetriene, A. Ibelhauptaite, and L. Staciokiene, "Phototransformation of sensitisers: 3. Implications for Clinical Dosimetry," *Lasers Surg. Med.* **13**, 271–278 (1998).
4. A. Curnow, J. C. Haller, and S. G. Bown, "Oxygen monitoring during 5-aminolaevulinic acid induced photodynamic therapy in normal rat colon: Comparison of continuos and fractionated light regimes," *Photochem. Photobiol.* **58**, 149–155 (2000).
5. S. Muller, H. Walt, D. Dobler-Girdziunaite, D. Fiedler, and U. Haller, "Enhanced photodynamic effects using fractionated laser light," *Photochem. Photobiol.* **42**, 67–70 (1998).
6. B. C. Wilson and M. S. Patterson, "The physics of photodynamic therapy," *Phys. Med. Biol.* **31**(4), 327–360 (1986).
7. W. Beyer, "Systems for light applicator and dosimetry in photodynamic therapy," *Photochem. Photobiol.* **36**, 153–156 (1996).
8. L. H. P. Murrer, J. P. A. Marijnissen, and W. M. Star, "Improvements in the design of linear diffusers for photodynamic therapy," *Phys. Med. Biol.* **42**, 1461–1464 (1997).
9. B. J. Tromberg, L. O. Svaasand, M. K. Fehr, S. J. Madsen, P. Wyss, B. Sansone, and Y. Tadir, "A mathematical model for light dosimetry in photodynamic destruction of human endometrium," *Phys. Med. Biol.* **41**, 223–237 (1996).
10. H. E. van Benthem, H. J. M. Sterenborg, F. W. van der Meulen, and M. J. C. van Gemert, "Performance of light applicator for photodynamic therapy in the oral cavity: calculations and measurements," *Phys. Med. Biol.* **42**, 1689–1700 (1997).
11. S. L. Jacques, "Simple theory, measurement and rules of thumb for dosimetry during photodynamic therapy," *Proc. SPIE* **1065**, 100–108 (1989).
12. L. I. Grossweiner, "PDT light dosimetry revisited," *Photochem. Photobiol.* **38**, 258–268 (1997).
13. J. P. A. Marijnissen, W. M. Star, H. J. A. Zandt, M. A. D. Hallewin, and L. Baert, "*In situ* light dosimetry during whole bladder wall photodynamic therapy: clinical results and experimental verification," *Phys. Med. Biol.* **38**, 567–582 (1993).
14. W. M. Star, "Light dosimetry *in vivo*," *Phys. Med. Biol.* **42**, 763–787 (1997).
15. O. Barajas, A. M. Ballangrud, G. G. Miller, R. B. Moore, and J. Tulip, "Monte Carlo modelling of angular radiance in tissue phantoms and human prostate: PDT light dosimetry," *Phys. Med. Biol.* **42**, 1675–1687 (1997).
16. W. F. Cheong, S. A. Prahl, and A. J. Welch, "A review of the optical properties of biological tissues," *IEEE J. Quantum Electron.* **26**, 2166–2185 (1990).